Ceramics International 32 (2006) 673–677

CERAMICS INTERNATIONAL

www.elsevier.com/locate/ceramint

Preparation of MgO-coated $BaTiO_3$ particles through a surface-induced precipitation method

Jae Sung Park, Young Ho Han *

Department of Materials Engineering, Sungkyunkwan University, 300 Chunchun-dong, Jangan-gu, Suwon 440-746, Republic of Korea

Received 5 January 2005; received in revised form 11 April 2005; accepted 9 May 2005
Available online 25 July 2005

Abstract

The effect of particle size of $BaTiO_3$ on the preparation of magnesia-coated $BaTiO_3$ particles was studied through a surface-induced precipitation method. MgO-coated $BaTiO_3$ particles were prepared by a homogeneous precipitation method using $MgCl_2{\cdot}6H_2O$ and urea. Particle sizes of starting $BaTiO_3$ powders were ~30 and ~400 nm, respectively. Amorphous magnesia precursor with ~10 nm was heat treated and transformed to crystalline MgO. Crystallization of MgO was observed at the temperature range between 600 and 700 °C. Zeta potentials were all negative such as −2 mV for MgO, −18 mV for 400 nm $BaTiO_3$ and −22 mV for 30 nm $BaTiO_3$ at pH 7.0. The MgO-coating layer was observed on $BaTiO_3$ particles with ~400 nm, whereas none of the coating layer was observed on $BaTiO_3$ with ~30 nm. According to calculation of the total interaction potential energy, the most strong attraction energy was observed between 400 nm $BaTiO_3$ and MgO particles.

Keywords: $BaTiO_3$; Mg; Homogeneous precipitation; Coating; Hetero-coagulation

1. Introduction

$BaTiO_3$ has been used as a basic ferroelectric material for electronic components such as multilayer ceramic capacitor (MLCC), PTC thermistors and sensors. Dielectric layers of MLCC are fabricated by tape casting of suspension with $BaTiO_3$ and oxide additives in an organic solvent. As the thickness of ceramic layers decreases, a well-dispersed suspension of $BaTiO_3$ particles and oxide additives is essential. In most cases, the mixing of additives in a ceramic system has been carried out by mechanical means. However, those methods have shown a critical success in dispersing additives homogeneously, compared with chemical mixing. To maximize the homogeneous distribution of additives, various chemical techniques such as sol–gel [1,2], hetero-coagulation [3–5] and homogeneous precipitation coating [6,7] have been studied recently.

In the conventional methods of adding a precipitant as a base to a reaction solution from outside, even a weak base added to the solution makes pH locally high. This leads to inhomogeneous chemical compositions with various impurities. On the other hand, the homogeneous precipitation method is one of the best methods to control the pH as well as to form pure and dense precipitates. The surface-induced precipitation is an application method of homogeneous precipitation. Matijevic reported that the uniform coating of inorganic shells on the inorganic cores is caused by surface reaction [8]. When precipitation of the coating material is uniformly distributed in the presence of suspended cores, a hetero-coagulation will occur under appropriate conditions with the performed particles to produce surface layers. Krishnan and Iwasaki studied the attachment of $Mg(OH)_2$ precipitates to quartz surface by hetero-coagulation and charge interaction between quartz and $Mg(OH)_2$ [9]. McLaughlin et al. reported a similar research on magnesium hydroxide and aluminum hydroxycarbonate that the development of an aluminum hydroxycarbonate coating on the magnesium hydroxide

---

* Corresponding author. Tel.: +82 31 290 7392; fax: +82 31 290 7410.
E-mail address: yhhan@yurim.skku.ac.kr (Y.H. Han).

0272-8842/$30.00 © 2005 Elsevier Ltd and Techna Group S.r.l. All rights reserved.
doi:10.1016/j.ceramint.2005.05.005

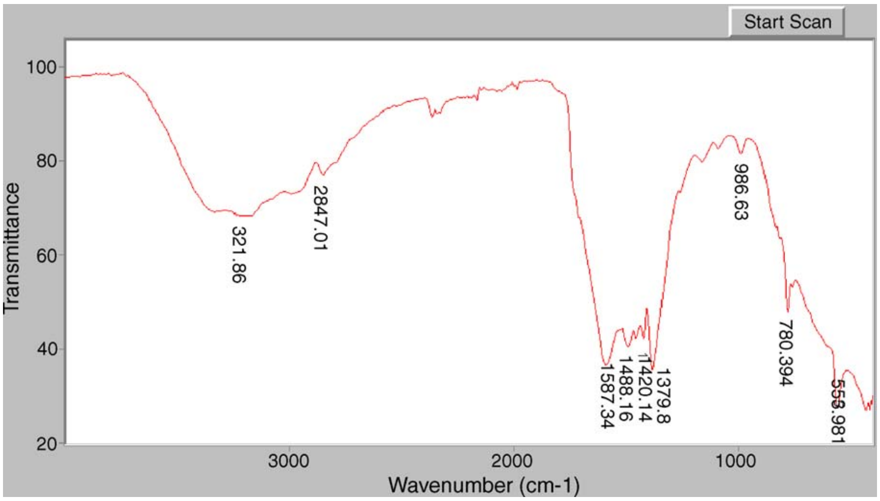

Fig. 1. FTIR analysis of precipitates formed by the reaction between $MgCl_2 \cdot 6H_2O$ and urea.

particles depends on zeta potentials of each particle in mixed suspensions [10,11].

In this study, a magnesia precursor was coated on the $BaTiO_3$ particles using a surface-induced precipitation technique and the effect of $BaTiO_3$ particle size on the hetero-coagulation between $BaTiO_3$ powder and magnesia precursor was studied.

2. Experimental procedure

$BaTiO_3$ powders with different particle sizes were used as core particles. $BaTiO_3$ powder with ~30 nm was prepared using the liquid mix method developed by Pechini [12] and Sakai BT-04 $BaTiO_3$ powder was used as ~400 nm core material. Reagent grade $MgCl_2 \cdot 6H_2O$ (99.99%, Aldrich) and urea (NH_2CONH_2 99%, Aldrich) were used for precipitating magnesium hydroxide from solution. All solutions and suspensions were prepared in distilled water. $BaTiO_3$ particles were suspended in distilled water and $MgCl_2 \cdot 6H_2O$ solution was added to the suspension with 1 M concentration urea. The suspension system was magnetically stirred with dispersant at room temperature and 80 °C for 1 and 2 h, respectively. The pH of the reaction mixture was increased up to 7.0 and then saturated. After stirring, the dispersion was aged at 90 °C for 12 h.

The crystalline phase of MgO precipitation was determined by X-ray diffraction analysis (Rigaku Rotaflex D/MAX System) and the formation of MgO surface coating was studied by a Fourier transform infrared spectroscopy (FTIR, Bruker IFS-66/S). The coated and uncoated $BaTiO_3$ powders were characterized by a transmission electron microscopy (TEM, Jeol-300kV). Zeta potentials of the coated and uncoated $BaTiO_3$ and MgO precursor were measured as a function of pH using an electrophoretic light scattering spectrophotometer (ELS-8000, Otsuka).

3. Results and discussion

Fig. 1 shows FTIR analysis of MgO precursor in the absence of $BaTiO_3$ powder. The intense bands at 1380 and 1488 cm^{-1} are assigned to carbonate bands partially bonded to Mg ion and the wide band observed at 3000–3600 cm^{-1} is assigned to hydroxyl group. Urea decomposes in the solution and increases pH, according to the following reaction [13]:

$$(NH_2)_2CO + 3H_2O \rightarrow CO_2 + 2NH_3 + 2H_2O \qquad (1)$$

The decomposition of urea gives rise to ammonia and carbon dioxide in the solution. Consequently, OH^- and CO_3^{2-} ions induce the precipitation of metal hydroxides and hydroxycarbonates, resulting in formation of precipitates. The precursor of magnesia would be precipitated through the hydrolysis reaction of urea, the uniform precipitations of

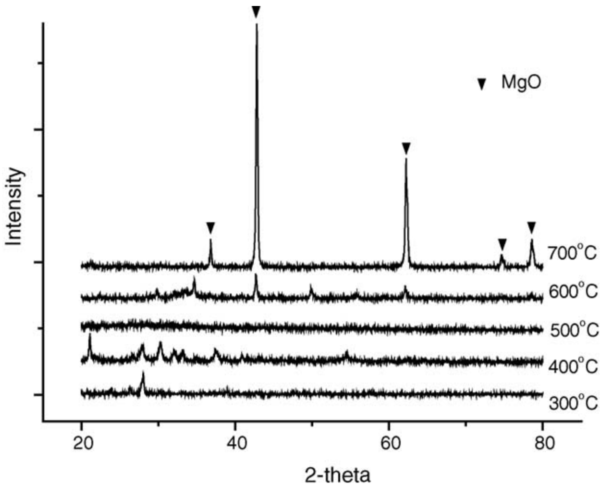

Fig. 2. XRD patterns of Mg precursor powder separately precipitated from $MgCl_2 \cdot 6H_2O$ solution with various heating temperatures.

magnesia precursor in the presence of $BaTiO_3$ particles leading to the hetero-coagulation which produced homogeneous distribution of additives on the $BaTiO_3$ surface.

Fig. 2 shows X-ray diffraction patterns of as-prepared MgO powders after heat treatment at 300–700 °C for 1 h. None of crystalline phase was formed below 600 °C and MgO phase was detected at the temperature higher than 600 °C. It was confirmed that magnesium hydroxide and carbonate were completely transformed into a crystalline MgO at about 700 °C.

Fig. 3 shows zeta potentials of $BaTiO_3$ powders and MgO precursor as a function of pH value. The zeta potentials of $BaTiO_3$ powders decrease drastically between pH 3 and 4 and gradually tail off with increasing pH > 4, with a slight difference between particle sizes. However, MgO shows a monotonical decrease in zeta potentials with increasing pH and a switching IEP from positive to negative at pH 6. The isoelectric points (IEP) of $BaTiO_3$ powders and MgO precursors were observed at pH ~ 3 and at pH 6, respectively. Generally, the most obvious way to promote hetero-coagulation is that two components should have opposite charges, and the strong attraction energy is developed between two components under this condition. In this experiment, pH of the suspension was adjusted in the range of pH 3–6 to coat MgO precursor onto the surface of $BaTiO_3$ powder via the hetero-coagulation process. However, pH of $BaTiO_3$ suspension system must be adjusted to greater than 7 for $BaTiO_3$, to avoid the dissolution of Ba^{2+} ions in acidic solution. Thus, pH of the suspension was adjusted to 7. Under this condition, the zeta potentials of MgO and $BaTiO_3$ powders were −2 mV (MgO), −18 mV (~400 nm $BaTiO_3$) and −22 mV (30 nm $BaTiO_3$), respectively.

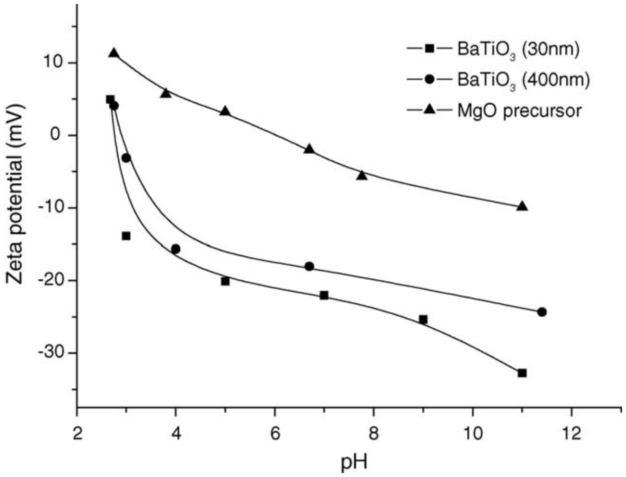

Fig. 3. Zeta potentials of $BaTiO_3$ and MgO particles as a function of pH values.

(a) 30nm $BaTiO_3$

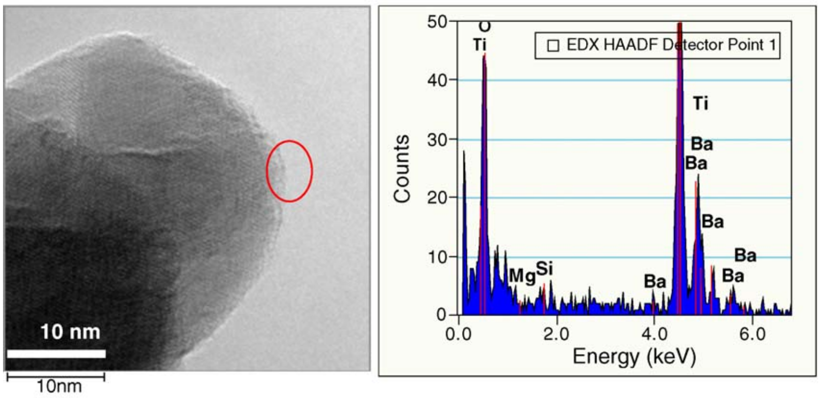

(b) 400nm $BaTiO_3$

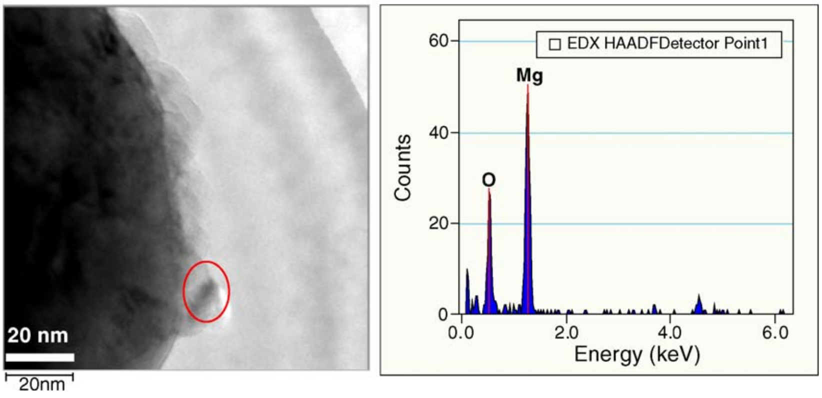

Fig. 4. TEM images of MgO-coated $BaTiO_3$ particles with different sizes: (a) 30 nm $BaTiO_3$; (b) 400 nm $BaTiO_3$.

Fig. 4 shows TEM images and EDS spectra of $BaTiO_3$ particles coated with MgO precursor, where the specimen was heat treated at 700 °C. MgO-coating layer was obviously observed on the surface of ∼400 nm $BaTiO_3$ powders. However, none of the electrostatic adsorption of MgO particles was detected on the surface of 30 nm $BaTiO_3$. Hetero-coagulation is affected by various parameters such as the concentration of particles, the relative numbers of the component particles, the relative surface charge and the relative particle size [14,15]. Most important parameters are the surface charge of the component particles and the particle size ratio between the component particles. Furusawa and Velev reported that the amount of uniform hetero-coagulate particles in the suspension increases with the increase of particle size ratio in the hetero-coagulation behavior of polymer lattices and spherical silica [14]. In the case of 400 nm $BaTiO_3$ and MgO system, the suspension comprised uniform hetero-coagulated particles (MgO-coated $BaTiO_3$). However, precipitated MgO precursor and 30 nm $BaTiO_3$ were composed of irregular aggregated particles because total interaction energy of $BaTiO_3$–$BaTiO_3$, $BaTiO_3$–MgO and MgO–MgO was similar to each other. According to DLVO theory, the attraction energy increases with increasing the relative particle size ratio, which is an important factor associated with hetero-coagulation. Thus, the different hetero-coagulation between $BaTiO_3$ and MgO shown in Fig. 4 could be due to the different relative particle size ratio between $BaTiO_3$ and MgO powder instead of the relative difference in the zeta potential. Fig. 5 shows the zeta potential of MgO-coated $BaTiO_3$ and uncoated $BaTiO_3$ as a function of pH. Between pH 3 and 10, MgO-coated $BaTiO_3$ exhibits slightly greater zeta potentials than the uncoated one. This indicates that MgO-coating modifies $BaTiO_3$ surfaces and develops relatively greater positive charge on the coating layer than the uncoated one.

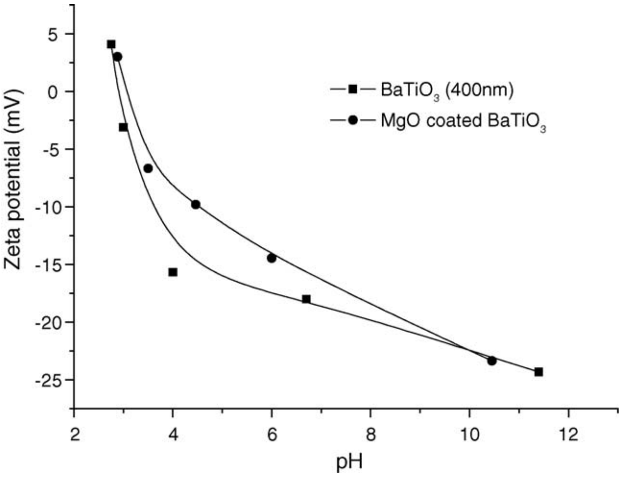

Fig. 5. Zeta potentials of uncoated and MgO-coated $BaTiO_3$ particles.

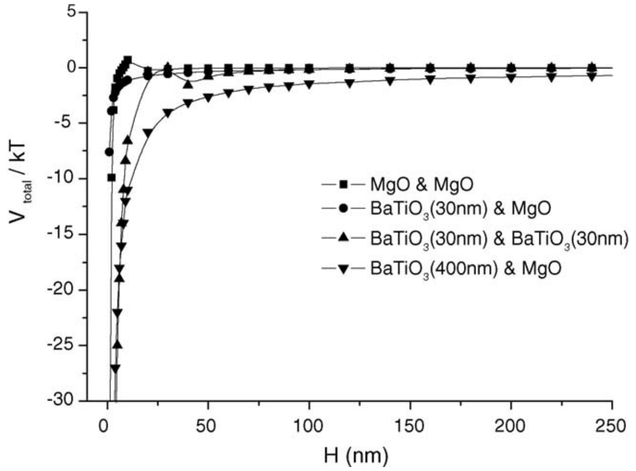

Fig. 6. Total interaction potential curves between MgO–MgO, $BaTiO_3$–MgO and $BaTiO_3$–$BaTiO_3$ at pH 7.0.

The total interaction potential energy curves between $BaTiO_3$–MgO, $BaTiO_3$–$BaTiO_3$ and MgO–MgO particles in the aqueous suspension are calculated according to the Derjaguin–Landau–Verwey–Overbeek (DLVO) theory [15,16] and plotted in Fig. 6.

The total interaction potential energy between pairs of identical oxides is given by

$$V = V_R + V_A \tag{2}$$

The repulsive energy as a function of particle separation (H) and the van der Waals energy of attraction for spheres of radius (a) with center-to-center distance (r) is

$$V_R = \pi a 64 n^\circ kT \left(\tanh \frac{ze\Psi_0}{4kT}\right)^2 \frac{1}{\kappa^2} \exp(-\kappa H) \tag{3}$$

and the attraction energy is given as

$$V_A = -A_{131} \frac{1}{6}\left(\frac{2}{s^2-4} + \frac{2}{s^2} + \ln\frac{s^2-4}{s^2}\right) \tag{4}$$

where κ, the Debye parameter is given by $\kappa = (2e^2 n^\circ z^2/\varepsilon_0 \varepsilon_r kT)^{1/2}$.

In the above equations, ε_0 is the dielectric permittivity of a vacuum, ε_r the relative dielectric constant of the medium, e the elementary charge, Z is the valence of the ion, n° is the bulk ion concentration, k is the Boltzmann constant, T the absolute temperature of the suspension, and Ψ_0 is the surface potential of the particle (here, $\Psi_0 = \zeta$, the zeta potential), $s = r/a$ and A_{131} is the effective Hamaker constant. The values of the Hamaker constants are 18×10^{-20} J ($BaTiO_3$), 12.1×10^{-20} J (MgO) and 4.83×10^{-20} J (water) [16,17].

Hogg et al. have extended the DLVO theory to include the interaction between spherical colloidal particles of different radii and having unequal surface potential, or different

Hamaker constants as follow [18]:

$$V_R = \frac{\pi\varepsilon_0\varepsilon_r a_1 a_2(\Psi_1^2+\Psi_2^2)}{(a_1+a_2)} \times \left\{ \frac{2\Psi_1\Psi_2}{\Psi_1^2+\Psi_2^2} \ln\frac{1+\exp(-\kappa H)}{1-\exp(-\kappa H)} + \ln[1-\exp(-2\kappa H)] \right\} \quad (5)$$

$$V_A = -\frac{A_{132}}{12}\left[\frac{y}{x^2+xy+x} + \frac{y}{x^2+xy+x+y} + 2\ln\left(\frac{x^2+xy+x}{x^2+xy+x+y}\right)\right] \quad (6)$$

where $x = H/(a_1 + a_2)$, $y = a_1/a_2$ and $A_{132} = 2.62 \times 10^{-20}$ J for $BaTiO_3$–water–MgO.

The total interaction potential energy curves are plotted in Fig. 6 for $BaTiO_3$ powder–MgO system at pH 7.0. A stronger attraction energy developed between $BaTiO_3$ (400 nm) and MgO particles and a hetero-coagulation would occur predominantly rather than in the system $BaTiO_3$ (30 nm)–MgO. The total interaction energy of $BaTiO_3$ (30 nm)–MgO system was similar to $BaTiO_3$–$BaTiO_3$ and MgO–MgO because of the relative particle size ratio, which is lower than 400 nm $BaTiO_3$–MgO. It implies that the probability of the hetero-coagulation of $BaTiO_3$ (30 nm)–MgO was abruptly reduced, resulting in irregular aggregates of powders.

4. Conclusion

MgO-coated $BaTiO_3$ particle was prepared from $BaTiO_3$ and $MgCl_2{\cdot}6H_2O$ by a homogeneous precipitation method using urea. The precipitation of Mg hydroxide was transformed to MgO between 600 and 700 °C. The zeta potential of $BaTiO_3$ and Mg precursor were −2 mV (MgO), −18 mV (400 nm $BaTiO_3$) and −22 mV (30 nm $BaTiO_3$) at pH 7.0, respectively. The Mg coating layer was observed on 400 nm $BaTiO_3$ particles, whereas none of MgO phase was observed on 30 nm $BaTiO_3$. According to calculation of the total interaction potential energy (DLVO theory), the most strong attraction energy was observed between 400 nm $BaTiO_3$ and MgO particles.

Acknowledgements

This research was supported by a grant from the Center for Advanced Materials Processing (CAMP) of the 21st Century Frontier R&D Program funded by the Ministry of Commerce, Industry and Energy (MOCIE), Republic of Korea.

References

[1] F.A. Selmi, V.R.W. Amamrakoon, J. Am. Ceram. Soc. 71 (1988) 934.
[2] W.-H. Shih, D. Kisailus, Y. Wei, Mater. Lett. 24 (1995) 13.
[3] R.D. Harding, J. Colloid Interface Sci. 40 (3) (1972) 164.
[4] T.W. Healy, G.R. Wiese, D.W. Yates, B.V. Kavangh, J. Colloid Interface Sci. 42 (3) (1973) 647.
[5] J.H. Jean, S.M. Yang, J. Am. Ceram. Soc. 83 (8) (2000) 1928.
[6] B.K. Kim, I. Yasui, J. Mater. Sci. 23 (1988) 637.
[7] B. Aiken, W.P. Hsu, E. Matijevic, J. Mater. Sci. 25 (1990) 1886.
[8] E. Matijevic, Langmuir 10 (1) (1994) 8.
[9] S.V. Krishnan, I. Iwasaki, Colloids Surf. 15 (1985) 89.
[10] W.J. McLaughlin, J.L. White, S.L. Hem, J. Colloid Interface 157 (1) (1993) 113.
[11] W.J. McLaughlin, J.L. White, S.L. Hem, J. Colloid Interface 167 (1) (1994) 74.
[12] M.P. Pechini, U.S. Patent 3,330,697 (1967).
[13] F. Boschini, B. Robertz, A. Rulmont, R. Cloots, J. Eur. Ceram. Soc. 23 (2003) 3035.
[14] K. Furusawa, O.D. Velev, Colloids Surf. A 159 (1999) 359.
[15] A.M. Islam, B.Z. Chowdhry, M.J. Snowden, Adv. Colloid Interface Sci. 62 (1995) 109.
[16] G. Wang, P.S. Nicholson, J. Am. Ceram. Soc. 84 (6) (2001) 1250.
[17] L. Bergstrom, Adv. Colloid Interface Sci. 70 (1997) 125.
[18] R. Hogg, T.W. Healy, D.W. Fuerstenau, Trans. Faraday Soc. 62 (1966) 1638.